RIVM Farm Building Study

ADMS Pitched Roof Module Development

1 Introduction

Cambridge Environmental Research Consultants (CERC) develop and licence ADMS, which is a world-leading, new generation, advanced Gaussian atmospheric dispersion model. This report describes the development of a prototype pitched-roof module within ADMS, with the aim of improving the prediction of concentrations downwind of an isolated pitched-roof building. This extends the present buildings module in ADMS, which was developed based on theoretical considerations and experimental measurements of flow and dispersion around cuboid buildings.

Section 2 presents a review of the relevant literature on flow and dispersion characteristics around pitched-roof buildings. Section 3 presents the methodology for the new prototype pitched-roof module in ADMS. In Section 4, the updated buildings module is validated against a wind tunnel concentration dataset that includes both flat-roof (Section 4.1) and pitched-roof (Section 4.2) building configurations. Finally, conclusions are drawn and future work discussed in Section 5.

2 Literature review

A literature search was performed on the flow and dispersion around pitched roof buildings.

There have been many studies relating to the effects of pitched roofs on flow within urban environments. These include studies that consider parallel street canyons, e.g. Yassin et al. (2022) who performed wind tunnel experiments and Reynolds-averaged Navier-Stokes (RANS) simulations, Ferrari et al. (2019) who performed water-channel experiments with Digital Image Analysis, and Wen and Malki-Epshtein (2018) who performed RANS simulations, as well as studies considering arrays of building, e.g. Coburn et al. (2022), who used a Large Eddy Simulation (LES) model.

Conversely, relatively few studies have considered isolated pitched roof buildings that are more typical of rural environments. Even among these studies, the focus is typically on determining roof-surface pressure fields/wind loads in order to assess wind damage potential, and less on the effect of pitched roofs on pollutant dispersion, e.g. Oliveira and Younis (2000) who used two RANS approaches to compare suction pressures against full-scale experimental data, and Hu et al. (2011) who used a tornado simulator with a digital Particle Image Velocimetry (DPIV) system to measure wind loads.

Using DPIV in a water channel, Sousa and Pereira (2004) showed that the inclusion of a gable roof on an isolated cubic obstacle had a significant influence on the mean flow and turbulence fields.

Ozmen et al. (2016) studied three roof pitch angles (i.e. the angle the roof makes with the horizontal) of 15°, 30° and 45° for an isolated gable-roof building in ‘perpendicular-to-apex’ flow, using wind tunnel experiments and two different Reynolds-averaged Navier-Stokes (RANS) models. They found that the flow structure around the building was highly influenced by the roof pitch angle. For the lowest pitch angle, the recirculation region behind the building was seen to separate downstream of the roof apex, while for the higher pitch angles, separation occurred at the apex itself and the recirculation region depth increased with increasing pitch angle. The lower pitch angle was shown to cause the highest pressure loads on the roof.

The RANS simulations of Tominaga et al. (2018) suggest that for winds perpendicular to the apex of an isolated gable-roof building, there is a critical roof pitch angle of approximately 20°:

- above which the flow separates from the roof apex, but
- below which the roof flow remains attached until the downwind edge of the building.

While the critical roof pitch angle is likely to be affected by factors such as the upstream surface roughness/turbulence intensity, the critical angle reported by Tominaga et al. (2018) is similar to the value found by Xing et al. (2018) in their investigations of isolated gable-roof buildings using wind tunnel tests, RANS and LES, and similar to the critical angle between a single and double vortex regime in an urban street canyon as reported by Takano and Moonen (2013). **Figure 1** is a reproduction of Fig. 12 from Tominaga et al. (2018) showing modelled streamlines for different roof pitches. The results indicate that for the roof pitch angles greater than the critical angle, the maximum height of the recirculation region behind the building increases with increasing pitch angle, with the top edge of the recirculation region initially following the approximate trajectory of the projected upwind roof slope before curving downwards with increasing downwind distance. Interestingly, the downwind extent of the recirculation region does not vary significantly between the various roof pitch angles modelled; it is between 2.5-2.8 times the roof base height from the downwind building wall in all modelled cases. The authors suggested this was due to the effect of increasing turbulent kinetic energy (and thus dissipation) at the upper wake edge with increasing pitch angle.

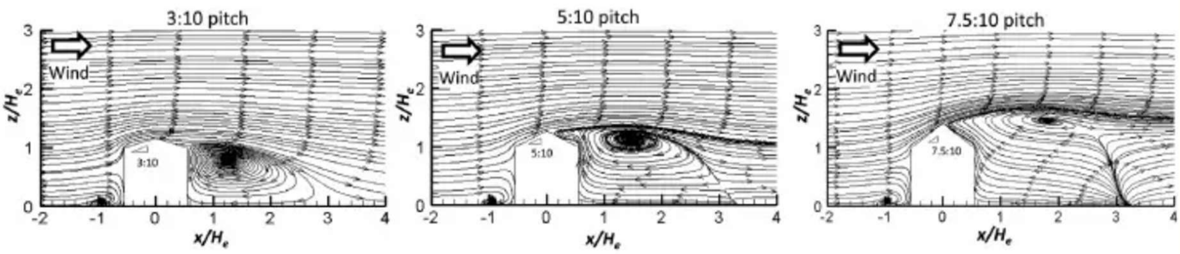

Figure 1 – Fig. 12. from Tominaga et al. (2018) showing streamlines for different roof pitches

Xing et al. (2018) also considered other wind directions and found that, conversely to perpendicular-to-apex flow, the flow was largely unaffected by the roof pitch angle for parallel-to-apex winds.

In terms of the effect of pitched roofs on pollutant dispersion, the literature again largely focuses on urban environments. The RANS simulations of Wen and Malki-Epshtein (2018) suggested that pitched roofs generally increase pollution concentration within street canyons due to reduced ventilation and lower velocities and turbulence within the canyon. The wind tunnel experiments and RANS simulations of Yassin et al. (2022) also showed higher in-canyon pollutant concentrations when comparing a pitched-roof configuration with a flat-roof one. Takano and Moonen (2013), however, found from their numerical modelling that for roof slopes below the critical angle between a one- and two-vortex regime, a steeper roof actually led to lower in-canyon concentrations.

To the authors' knowledge, the only publication focussing on the measurement of dispersing pollutants around an *isolated* gable-roof building is that of Potma et al. (2012). In this study, wind tunnel experiments conducted by the Dutch engineering consultancy Peutz were performed in which a tracer was released from the middle of the apex of a gable-roof obstacle (building) representing a livestock barn, with a roof pitch angle of 22.6°. The wind tunnel was equipped with 21 near-ground-level receptors, located along three separate lines extending away from the building; time-averaged tracer concentrations across multiple wind directions were recorded. Consistent measurements were also recorded corresponding to a flat-roof building with roof height equal to the maximum (apex) height of the pitched-roof building. **Figure 2** has been plotted from the tabulated data in Appendix F of Potma et al. (2012) and shows how concentrations varied with downwind distance from the source for three different wind directions, for both the flat-roof and pitched-roof building configurations (and the ratio between them). For a perpendicular-to-apex wind direction (0°), the concentrations downwind of the pitched-roof building were very similar to those seen with the flat-roof building – see **Figure 2a**. This seems consistent with Tominaga et al. (2018), given that the roof pitch angle of 22.6° is greater than the 20° critical angle mentioned in that paper (thus separation is expected to occur from the apex), but sufficiently shallow that the recirculation region behind the building will be of a similar depth to that behind a flat-roof building of apex height. Near-building downwind concentrations for a parallel-to-apex wind direction (270°) were seen to increase by around 60 % compared with the flat-roof configuration (**Figure 2b**). The ratio for a diagonal-to-apex wind direction (315°) showed a more complicated pattern (**Figure 2c**): The concentration immediately downwind of the pitched-roof building was almost double that recorded immediately downwind of flat-roof building, suggesting streamlines bringing emitted material down the slope of the pitched roof (and thus no separation from the apex for this wind direction), while concentrations further downwind were then seen to fall slightly below the flat-roof values, other than at the receptor at around 100 m from the source where a striking local maximum was seen in the pitched-roof data. Potma et al. (2012) suggested this local peak was caused by the delayed grounding of the unentrained part of the plume, however the tabulated data in Appendix F of their report also shows a sharp increase in concentration at this receptor for other wind directions that cannot be as easily explained (e.g. 0°).

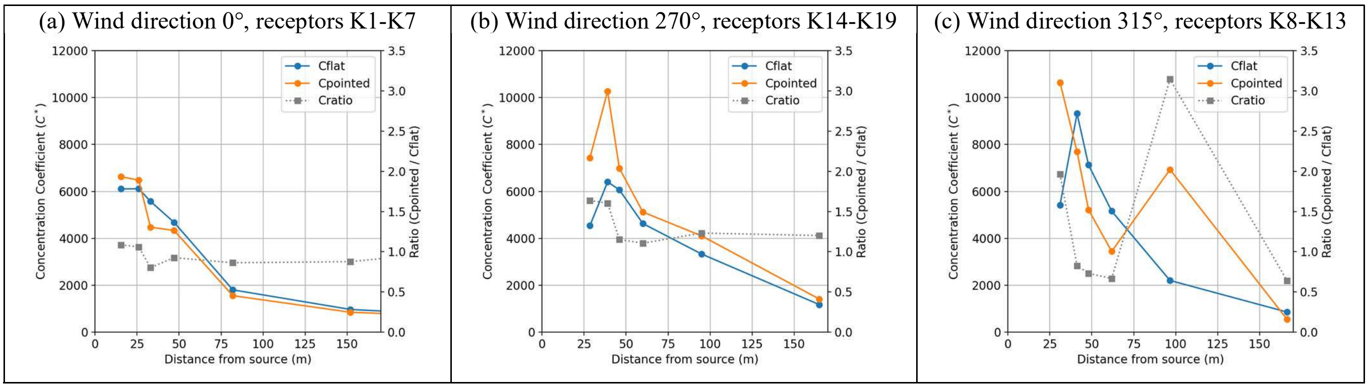

Figure 2 – Near-ground-level concentrations from the Peutz wind tunnel experiments downwind of the flat-roof building (blue line) and the pitched-roof building (orange line), and their ratio (grey line), for wind directions of (a) 0° (perpendicular-to-apex), (b) 270° (parallel-to-apex) and (c) 315° (diagonal-to-apex)

3 Methodology

The following section describes the methodology behind the prototype pitched roof module in ADMS 6.

The current ADMS 6 buildings module (Carruthers et al., 1994) takes one or more cuboidal or cylindrical buildings as input and, for each buildings-affected point source for each hour of meteorological data, generates a single wind-aligned 'effective' building of fixed height. A parameterised flow field around this effective building is then determined, including a recirculation region behind the building and turbulent wake further downstream. Plume dispersion calculations are performed using this flow field, including the calculation of the fraction of the plume entrained into the recirculation region.

For consistency, the new pitched-roof development continues to use this general approach, i.e. a pitched-roof building will still be modelled as a wind-aligned flat-roof building. However, it applies an adjustment of the effective building height and effective source height for a given wind-to-apex angle, using the data on impacts of pitched roofs on the flow field presented in Section 2. In the following, we refer to the pitched-roof building as the 'real' building and the flat-roof building that is actually modelled for a particular source and met. hour as the 'effective' building.

3.1 Wind perpendicular to apex

Effective building height

When the wind is perpendicular to the apex of the pitched roof, the effective building height H_B is based on the roof pitch angle γ:

$$H_B = \begin{cases} H_{\text{base}} & \gamma \leq \gamma_{\text{crit}} \\ H_{\text{apex}} & \gamma > \gamma_{\text{crit}} \end{cases}$$

where H_{base} is the roof base height and H_{apex} is the apex height. For the critical roof pitch angle, we choose

$$\gamma_{\text{crit}} = 20°$$

following Tominaga et al. (2018). Although assumed here to be a constant value, in reality γ_{crit} will likely be dependent on the level of turbulence in the approach flow, as higher turbulence levels inhibit flow separation.

Recirculation region shape

When $\gamma \leq \gamma_{\text{crit}}$, the recirculation region cross-section remains unaltered from the standard ADMS buildings approach. When the roof flow reattaches, this is a horizontal quarter ellipse with its centre at the downwind base of the effective building and a half-height and half-length of H_B and H_R respectively – see the left panel in **Figure 3**. (When the roof flow remains separated, a slightly different centre point and half-height are used – see the buildings Technical Specification document for full details.)

When $\gamma > \gamma_{\text{crit}}$, the recirculation region cross-section is modified so that its depth increases with roof pitch angle – see the middle and right panels in **Figure 3**. We define a horizontal ellipse, with its centre at ground level, that passes through the following three points:

$$(x_1, z_1) = \left(-\frac{L_B}{2}, H_{\text{base}}\right)$$

$$(x_2, z_2) = \left(0, H_{\text{apex}}\right)$$

$$(x_3, z_3) = \left(\frac{L_B}{2} + H_R, 0\right)$$

where module coordinates have been used (origin at the ground centre of the effective building and x-axis in the direction of the mean wind), and L_B is the along-wind length of the effective building. Only the part of this ellipse that is above ground and downwind of the effective building centre is retained.

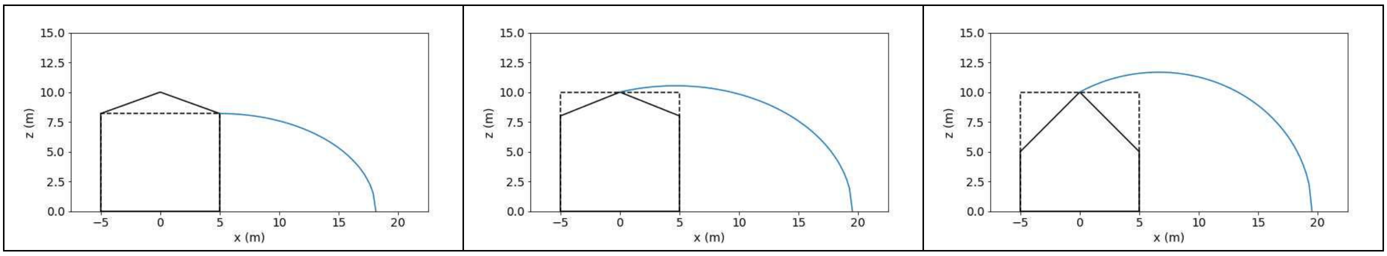

Figure 3 – Recirculation region cross section (blue line) for a roof pitch angle of 19.8° (left), 21.8° (middle) and 45° (right). Real and effective building outline shown by solid and dashed black lines, respectively.

Effective source height

For sources that are on/above the (real) building roof, the source height z_s is also potentially modified:

$$z_{s,\text{eff}} = \begin{cases} z_s & \gamma > \gamma_{\text{crit}} \text{ and } x_s > 0 \\ \text{H}_B + z_s - z_{\text{roof}} & \text{otherwise} \end{cases}$$

where z_{roof} is the height of the roof at the (horizontal) source location, and x_s is the x-coordinate of the source in module coordinates. This ensures a consistent distance between the effective building roof and the release point – the assumption here is that the streamlines directly above the pitched roof follow the slope of the roof in regions where the flow has not separated[1].

Note that an appropriate 'effective' source height is important for the calculation of C_R, which is taken to be the average concentration on the surface of the recirculation region (when the release is not fully entrained).

3.2 Wind parallel to apex

Effective building height

When the wind is parallel to the apex of the pitched roof, the effective building height H_B is

[1] The current prototype does not consider the case where flow separation occurs off the upwind edge of the building and does not reattach before the source location.

taken to be the half-roof height. That is:

$$H_B = \frac{H_{\text{base}} + H_{\text{apex}}}{2}$$

Recirculation region shape

The recirculation region cross-section remains unaltered from the standard ADMS buildings approach.

Effective source height

For sources that are on/above the (real) building roof, the source height is adjusted vertically to ensure a consistent distance between the effective building roof and the release point, i.e. $z_{\text{s,eff}} = \text{H}_B + z_s - z_{\text{roof}}$. If the source is moved closer to the ground, the contribution from the non-entrained part of the plume is only included outside the recirculation region (i.e. concentrations within the recirculation region will be equal to the uniform recirculation region concentration C_R) to avoid unrealistically large concentrations within this region.

3.3 Generalisation to any wind direction

To generalise the scheme to any wind direction, we calculate the effective roof pitch angle, γ_{eff}. This is the angle experienced by a streamline passing over the roof apex. This must be equal to γ for a perpendicular-to-apex wind and 0° for a parallel-to-apex wind. For intermediate wind directions, it takes the value:

$$\gamma_{\text{eff}} = \tan^{-1}(\tan\gamma \sin\phi_\Delta)$$

where ϕ_Δ is the acute angle between the roof apex and the wind – see **Figure 4**.

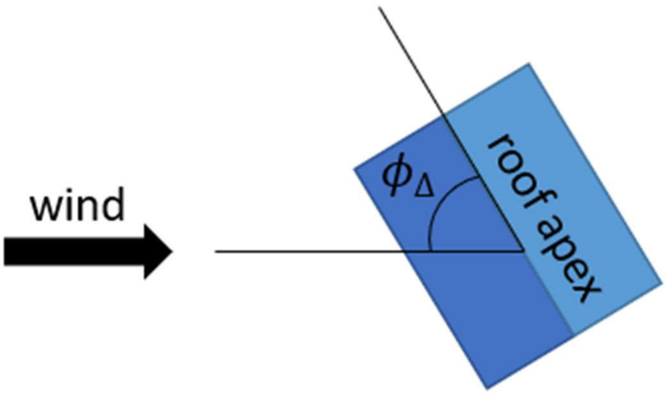

Figure 4 – Schematic diagram showing ϕ_Δ

When $\gamma_{\text{eff}} > \gamma_{\text{crit}}$, the same methodology is followed for perpendicular-to-apex winds with $\gamma > \gamma_{\text{crit}}$. That is, the height of the (wind-aligned) effective building is set to $H_B = H_{\text{apex}}$, the upper limit of the recirculation region is modified, and the height of any source in the upwind half of the effective building footprint is adjusted to ensure a consistent distance between the effective building roof and the release point, i.e. $z_{\text{s,eff}} = \text{H}_B + z_s - z_{\text{roof}}$.

When $\gamma_{\text{eff}} \le \gamma_{\text{crit}}$, the height of the effective building is set to the (average) roof height of the side of the building with the largest projected crosswind width. This will either be H_{base} or the half-roof height $(H_{\text{base}} + H_{\text{apex}})/2$. For sources that are on/above the (real) building roof, the source height is adjusted vertically to ensure a consistent distance between the effective building roof and the release point, i.e. $z_{\text{s,eff}} = \text{H}_B + z_s - z_{\text{roof}}$. If the source is moved closer to the ground, the contribution from the non-entrained part of the plume is only included outside the recirculation region.

4 Results and discussion

The Peutz wind tunnel dataset published in Potma et al. (2012) is used to validate the new pitched-roof module. As this dataset includes a flat-roof as well as a pitched-roof configuration, we first validate the 'standard' ADMS buildings module against the flat-roof data to check for general consistency between model outputs and the wind tunnel measurements.

4.1 Flat roof modelling

ADMS 6 was configured to mimic the (full-scale) flat-roof wind tunnel configuration, as follows:

- **Building dimensions**: 24 (L) x 50 (W) x 7 (H) m
- **Point source**: Height 7 m; diameter 1.05 m; exit velocity 0.1 m/s; ambient release; placed at the horizontal centre of the building; unit emission rate
- **Meteorology**: Surface roughness 0.03 m; wind speed at 10 m of 4.08 m/s; surface sensible heat flux of 0 W/m^2 (fully neutral); wind directions of 0° (normal to building width), 270° (normal to building length) and 315° (diagonal to building); lateral spread of 0° (i.e. no wind meandering), as appropriate when comparing atmospheric dispersion model outputs to wind tunnel measurements.
- **Receptor locations**: Match those used in the wind tunnel (all at z = 1.5 m)

Figure 5 compares the normalised concentrations from ADMS and the wind tunnel (WT) dataset for the three tested wind directions for the flat-roof configuration. In general, the model compares well with the WT data, particularly for the 0° (perpendicular-to-building-width) wind direction, for which the largest discrepancy occurs around 30 m downwind of the source with ADMS predicting a concentration ~30% higher than the WT value. The near-building concentrations also match up well for the 270° (perpendicular-to-building-length) wind direction, with ADMS predicting concentrations that are around 40% lower than the WT concentrations further downwind of the building. For the 315° (diagonal-to-building) wind direction, the ADMS concentrations are consistently around 20-30% lower than the WT concentrations downwind of the first receptor.

In general, concentrations predicted by a Gaussian model such as ADMS, which is based on similarly theory derived from measurements of the real atmospheric boundary layer, might be expected to be lower than 'equivalent' concentrations measured in a wind tunnel, where the physical restrictions of the wind tunnel itself prevent the generation of the largest scales of turbulence.

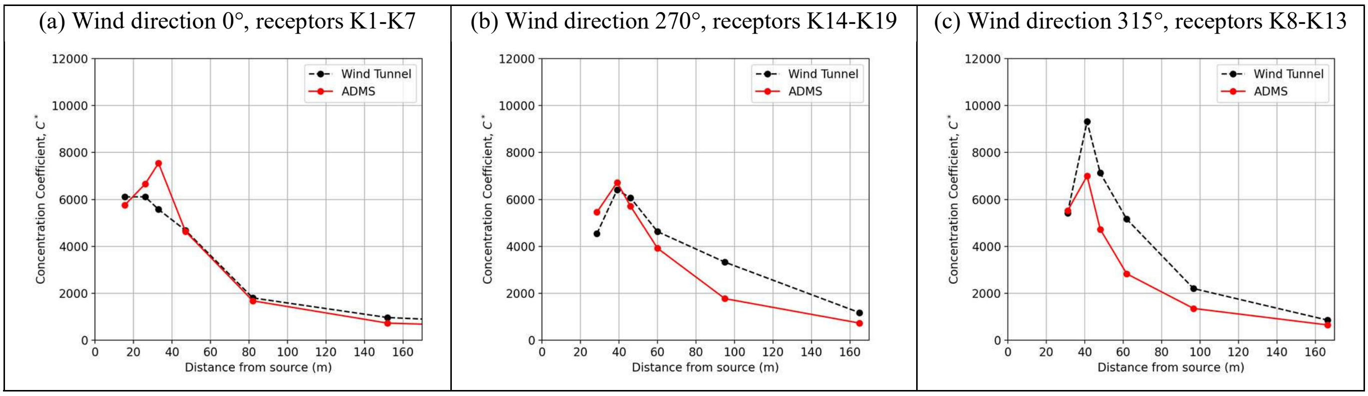

Figure 5 – ADMS vs Peutz WT normalised concentrations downwind of the flat-roof building for three different wind directions.

Figure 6 and **Figure 7** show horizontal and vertical normalised concentration contours from ADMS downwind of the flat-roof building for each of the three tested wind directions. These plots will be used for later comparison with modelled results from the pitched-roof configuration in Section 4.2.

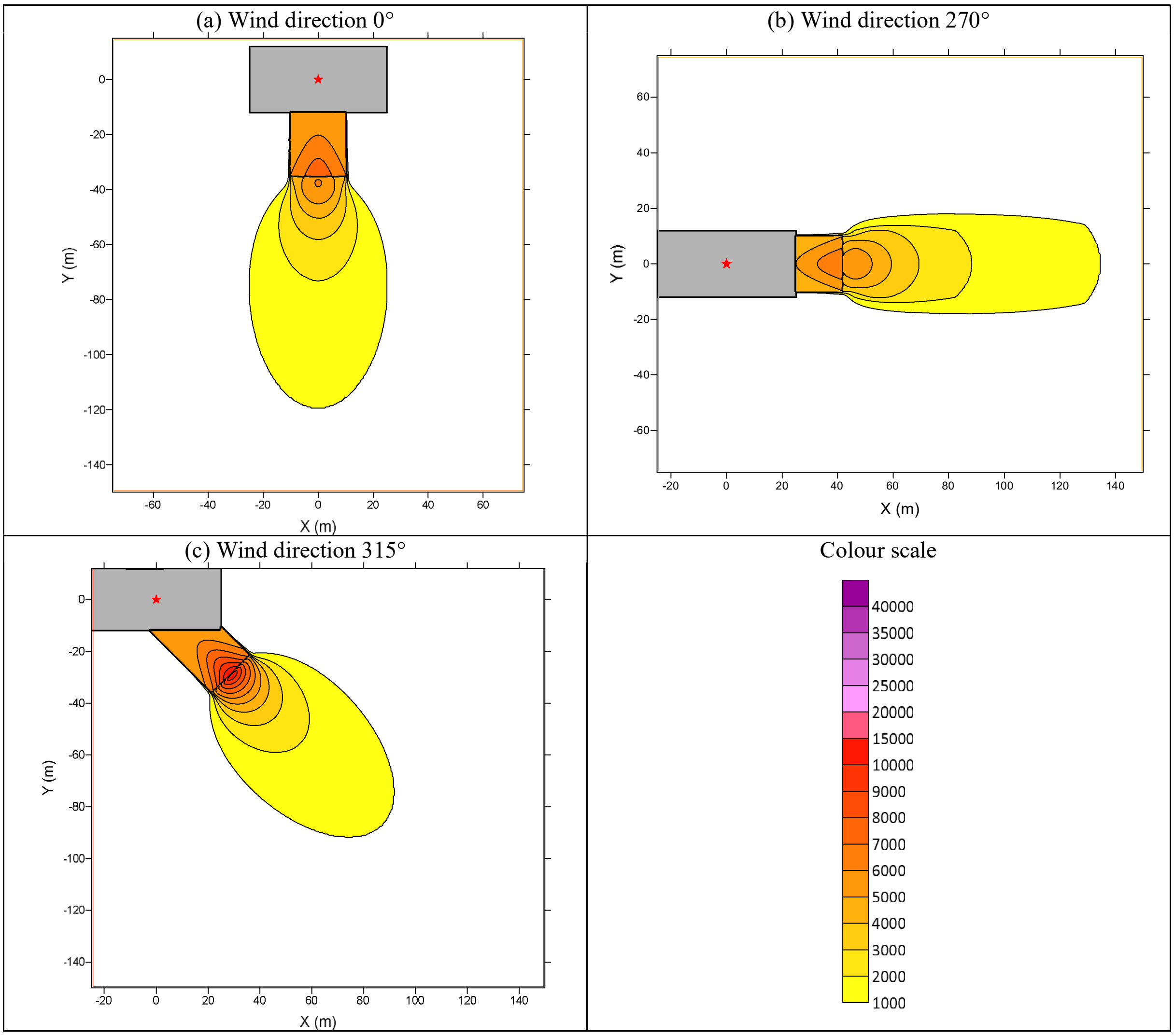

Figure 6 – ADMS normalised concentration contours at z = 1.5 m downwind of the flat-roof building (grey rectangle) for three different wind directions. Source location shown by red star.

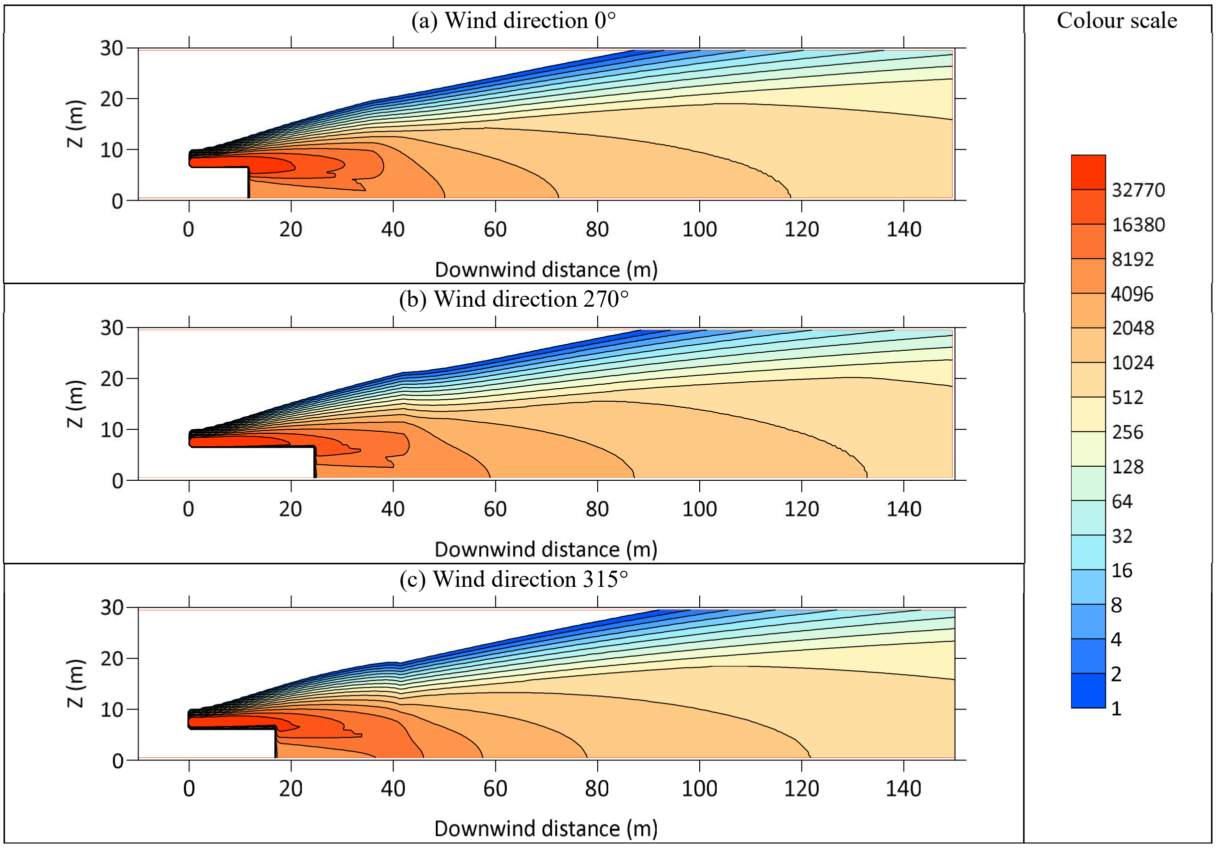

Figure 7 – Vertical slice ADMS normalised concentration contours downwind of the flat-roof building for three different wind directions. Vertical slice passes through the source and is oriented with the wind direction.

4.2 Pitched roof modelling

The modified version of ADMS 6 that includes the prototype pitched-roof module was then configured to mimic the (full-scale) pitched-roof wind tunnel configuration. This is the same model configuration as used for the flat-roof (Section 4.1), with the following exceptions:

- **Building dimensions**: The building height in the ADMS 'Buildings' screen was reduced from 7 m to the roof base height of the pitched roof building (2 m)
- **Pitched roof option**: The apex height of the pitched roof building was set to 7 m and the apex was specified as running parallel to the longest building edge; this information was passed in via a new additional input (*.aai*) file section.

Figure 8 compares the normalised concentrations from ADMS and the WT dataset for the three tested wind directions for the pitched-roof configuration.

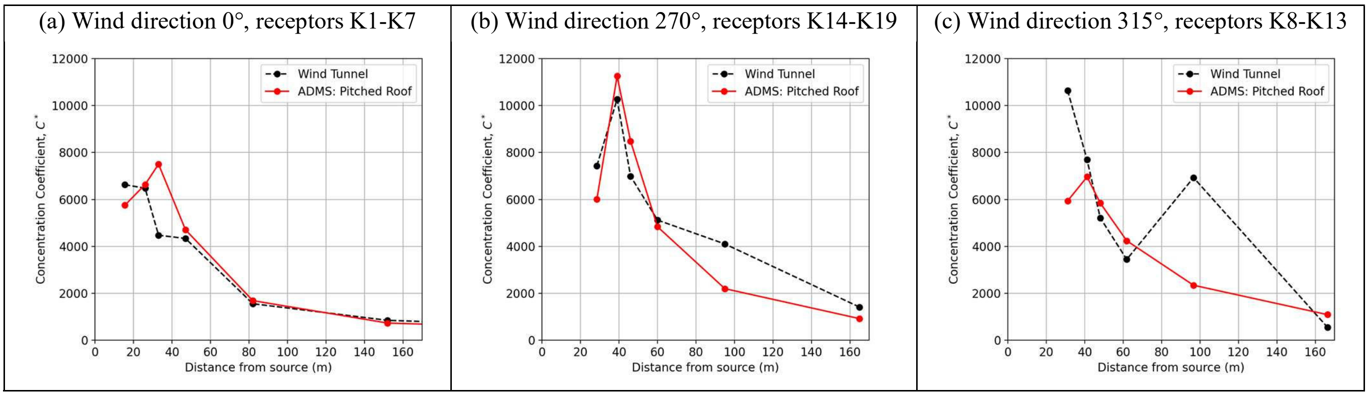

Figure 8 – ADMS vs Peutz WT normalised concentrations downwind of the pitched-roof building for three different wind directions.

For the 0° (perpendicular-to-apex) wind direction (**Figure 8a**), ADMS generally compares well against the WT data. This is as we might expect, given that it also compares well against the WT data for the flat-roof configuration in which the building height was equal to the apex height (see **Figure 5a**). Given that the roof pitch angle (22.6°) is greater than the critical angle (20°), ADMS models the pitched-roof building as a flat-roof building with height equal to the apex height. Thus, the only difference in the model between this configuration and the flat-roof configuration is the change to the shape of the recirculation region. This has little effect on modelled concentrations in this case, as the relatively shallow roof pitch angle leads to a recirculation region that has a similar depth to the one in the flat-roof configuration, as shown in **Figure 9**. As with the flat-roof configuration, the largest discrepancy between ADMS and the WT data occurs around 30 m downwind of the source, with the ADMS concentration now ~65 % higher than the WT value.

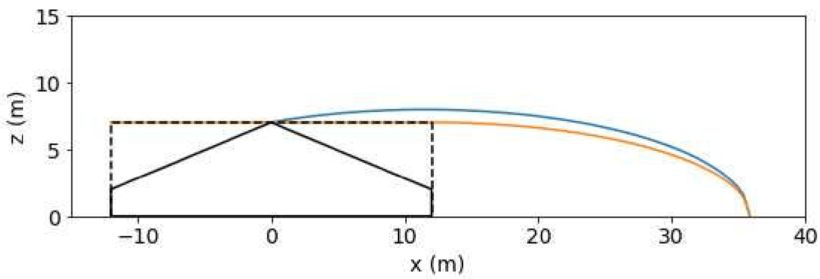

Figure 9 – ADMS recirculation region cross-section for the Peutz WT pitched-roof (blue line) and flat-roof (orange line) configurations for a perpendicular-to-apex wind direction. Pitched- and flat-roof building outline shown by solid and dashed black lines, respectively.

For the 270° (parallel-to-apex) wind direction (**Figure 8b**), both the WT and ADMS concentrations have increased in the near field compared with the flat-roof configuration (see **Figure 5b**), with the maximum concentration (which occurs at ~40 m downwind of the source) increasing by around 60-70 %. The match-up between ADMS and the WT data is good in the near-field, while ADMS predicts concentrations that are around 40-50% lower than the WT concentrations further downwind of the building. Similar differences were seen in the flat-roof configuration, suggesting that most of this difference is not attributable to the pitched-roof modifications themselves. For this wind direction, ADMS models the pitched-roof building as a flat-roof building with height equal to the half-roof height (4.5 m), as shown in **Figure 10**. The model also reduces the source height from 7 m to 4.5 m so that it remains at roof-level with respect to the effective building.

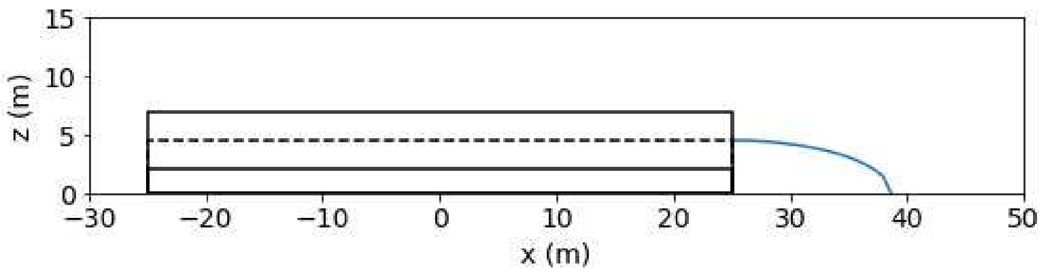

Figure 10 – ADMS recirculation region cross-section (blue line) for the Peutz WT pitched-roof configuration for a parallel-to-apex wind direction. Real and effective building outline shown by solid and dashed black lines, respectively.

For the 315° (diagonal-to-apex) wind direction (**Figure 8c**), the ADMS concentrations are generally higher than those seen with the flat-roof configuration (see **Figure 5c**), particularly at larger downwind distances, though the maximum near-field concentration at ~40 m does not change significantly. Conversely, the WT data shows an increase of around 100% at the first downwind receptor before then falling slightly below the equivalent flat-roof concentrations further downwind, apart from at ~100 m where a sharp increase in concentration occurs that is not seen in the flat-roof concentration data. As discussed in Section 2, the tabulated data in Appendix F of Potma et al. (2012) shows an extreme local maximum at this receptor for multiple wind directions, some of which cannot be easily explained (e.g. 0°), and so we feel that data from this receptor should be ignored. With this in mind, the WT and ADMS concentrations match reasonably well after the first downwind receptor. For this wind direction, $\phi_\Delta = 45°$ and thus the height of the wind-aligned effective building in ADMS is 2 m given that $\gamma_{\mathrm{eff}} < \gamma_{\mathrm{crit}}$ and the projected crosswind width of the side of the building with height H_{base} is twice that of the side of the building with variable roof height. The model also reduces the source height from 7 m to 2 m so that it remains at roof-level with respect to the effective building. Note that the receptors do not fall directly below the plume centreline for this wind direction.

Figure 11 and **Figure 12** show horizontal and vertical normalised concentration contours from ADMS downwind of the pitched-roof building for each of the three tested wind directions. The equivalent plots for the flat-roof configuration are shown in **Figure 6** and **Figure 7**. The flat-roof and pitched-roof concentrations for the 0° (perpendicular-to-apex) wind direction are similar throughout the domain, as expected. For the 270° (parallel-to-apex) wind direction, the increase in the recirculation region concentration with the pitched-roof configuration, and the concentrations downwind of this region, is evident. The vertical slice contours show that for the pitched-roof configuration, the very large concentrations close to the source are masked by the fact that ADMS does not output concentrations at points within the real building, which is taller than the effective building at the apex. *The pitched-roof module should therefore not be used if concentrations above the roof itself are required* (most modellers are interested in concentrations downwind of the building). For the 315° (diagonal-to-apex) wind direction, the near-building concentrations seen with the pitched-roof configuration are noticeably higher than those seen with the flat-roof configuration. The justification for this is that the downslope streamlines on the downwind half of the pitched roof will bring material down towards the ground, before flow separation then occurs only once the plume leaves the downwind (low) edge of the building. The wind tunnel receptors along the 315° measurement line (K8-K13) align with the corner of the building rather than being located directly under the plume centreline, and so none of these receptors fall within the ADMS recirculation region. However, there is a standalone receptor, K21, that does fall within this recirculation region, at which a normalised concentration of 8693 was recorded in the wind tunnel. The normalised recirculation region concentration predicted by ADMS is 14313; around 65% higher than the wind tunnel value.

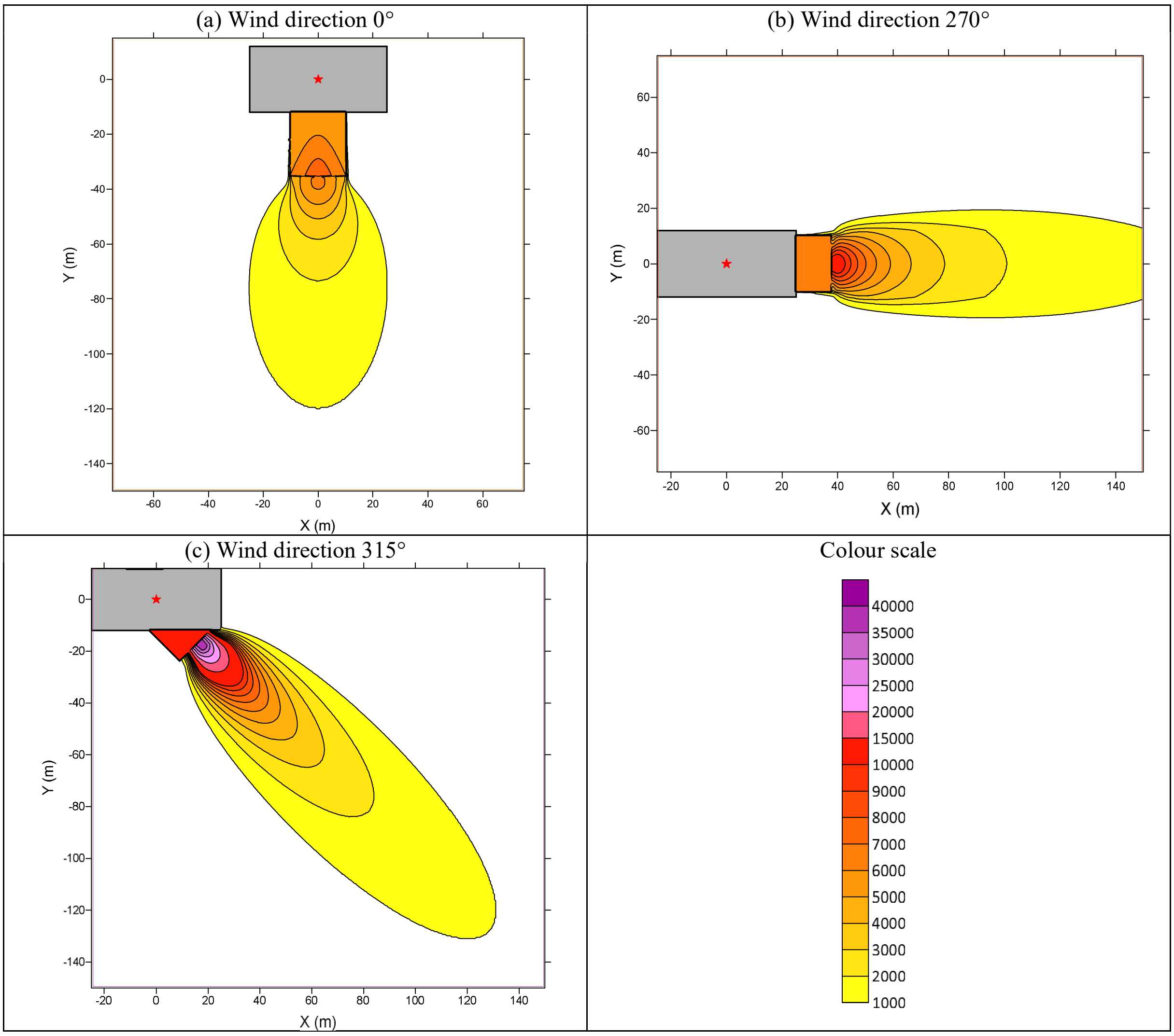

Figure 11 – ADMS normalised concentration contours at z = 1.5 m downwind of the pitched-roof building (grey rectangle) for three different wind directions. Source location shown by red star.

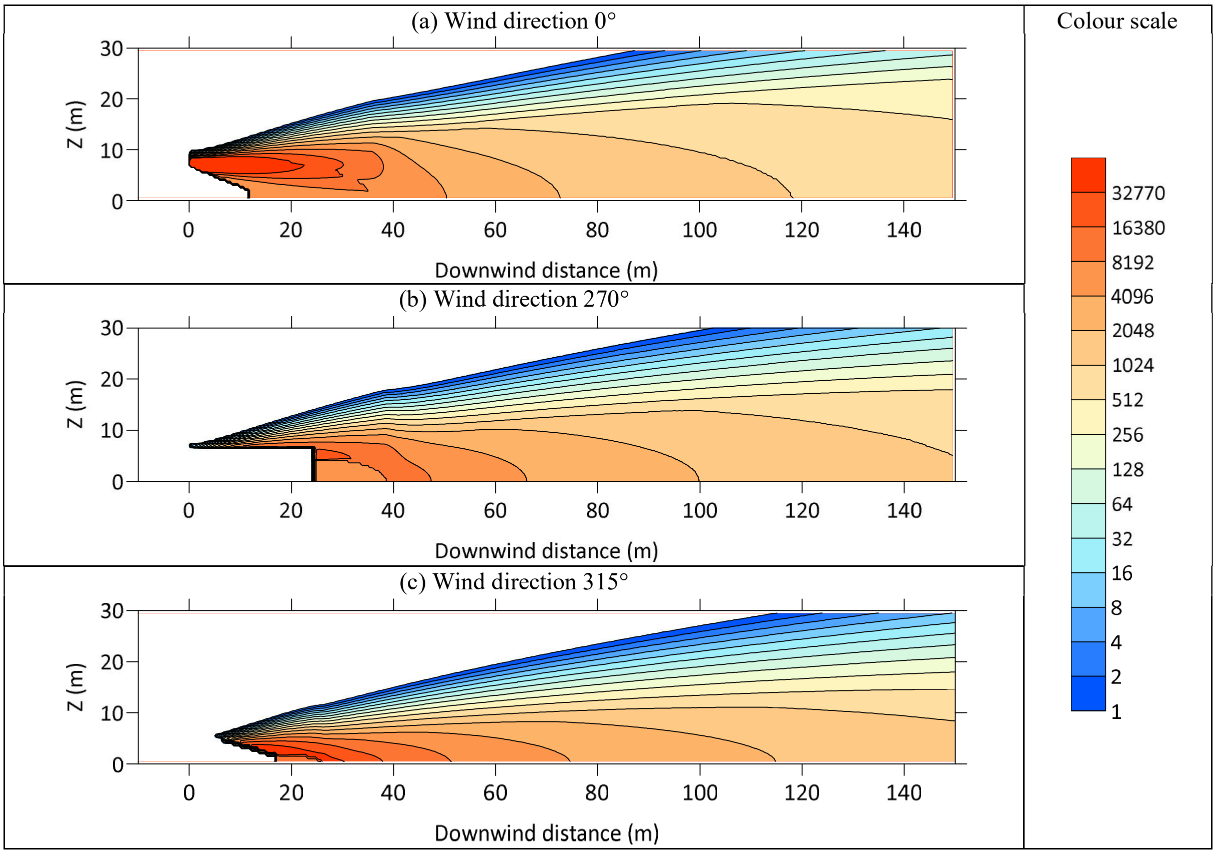

Figure 12 – Vertical slice ADMS normalised concentration contours downwind of the pitched-roof building for three different wind directions. Vertical slice passes through the source and is oriented with the wind direction.

5 Conclusions and future work

A development to the ADMS buildings module has been presented that aims to improve the prediction of concentrations downwind of an isolated pitched-roof building. The method modifies the height of the effective wind-aligned building and shape of the recirculation region depending on the roof pitch angle and the angle between the oncoming wind and the apex of the pitched-roof building, as well as potentially the source height to maintain the same relative height above roof level.

The new module validates reasonably well against a wind tunnel dataset in which a tracer was released from the middle of the apex of a gable-roof obstacle (building) with a single roof pitch angle (22.6°). Concentrations downwind of the pitched-roof building do not change significantly for a perpendicular-to-apex wind direction compared with concentrations downwind of a flat-roof building of apex height. While, for a parallel-to-apex wind direction, near-building concentrations are around 60-70 % higher than for the flat-roof building. Higher modelled downwind concentrations are also obtained for a diagonal wind for the pitched-roof building.

The prototype pitched-roof module shows good correspondence with the wind tunnel dataset presented, however the dataset is limited, so further testing needs to be undertaken before the module can be included in a release version of ADMS. Such testing would ideally include comparison against experiments and/or numerical modelling with different roof pitch angles, different source locations above the roof (not just on the apex) and different meteorological conditions/atmospheric stabilities, however there is little such data currently available.

The prototype pitched-roof module has the following assumptions/restrictions, which may also be addressed in future work:

- Only one input building may be defined, and this must be a rectangular building
- The roof apex is assumed to run down the middle of the building, i.e. it is only possible to model a single symmetrical gable roof building per simulation

References

Carruthers DJ, Holroyd RJ, Hunt JCR, Weng W-S, Robins AG, Apsley DD, Thompson DJ, Smith FB (1994) UK-ADMS: a new approach to modelling dispersion in the earth's atmospheric boundary layer. J Wind Eng Ind Aerodyn 52:139–153. https://doi.org/10.1016/0167-6105(94)90044-2

Coburn M, Xie Z-T, Herring S J (2022) Numerical Simulations of Boundary-Layer Airflow Over Pitched-Roof Buildings. Boundary-Layer Meteorol 185(3):415–442. https://doi.org/10.1007/s10546-022-00738-1

Ferrari S, Badas MG, Garau M, Salvadori L, Seoni A, Querzoli G (2019) On The Effect Of The Shape Of Buildings And Chimneystacks On Ventilation And Pollutant Dispersion. EPJ Web Conf., 213, 02017. https://doi.org/10.1051/epjconf/201921302017

Hu H, Yang Z, Sarkar P, Haan F (2011) Characterization of the wind loads and flow fields around a gable-roof building model in tornado-like winds. Exp Fluids 51:835–851. https://doi.org/10.1007/s00348-011-1102-6

Oliveira PJ, Younis BA (2000) On the prediction of turbulent flows around full-scale buildings. J Wind Eng Ind Aerodyn 86(2–3):203–220. https://doi.org/10.1016/S0167-6105(00)00011-8

Ozmen Y, Baydar E, van Beeck JPAJ (2016) Wind flow over the low-rise building models with gabled roofs having different pitch angles. Build Environ 95:63–74. https://doi.org/10.1016/j.buildenv.2015.09.014

Potma C, van den Akker A, van Ratingen S, Erbrink JJ, Kokmeijer E, Verhees E (2012) Herijking gebouwroutine: een analyse, validatie en voorstellen tot verbetering. 74101268-CES/ECS 12-7432. KEMA

Sousa JMM, Pereira JCF (2004) DPIV study of the effect of a gable roof on the flow structure around a surface-mounted cubic obstacle. Exp Fluids 37:409–418. https://doi.org/10.1007/s00348-004-0830-2

Takano Y, Moonen P (2013) On the influence of roof shape on flow and dispersion in an urban street canyon. J Wind Eng Ind Aerodyn 123(A):107–120. https://doi.org/10.1016/j.jweia.2013.10.006

Tominaga Y, Akabayashi S, Kitahara T, Arinami Y (2015) Air flow around isolated gable-roof buildings with different roof pitches: Wind tunnel experiments and CFD simulations. Build Environ 84:204–213. https://doi.org/10.1016/j.buildenv.2014.11.012

Wen H, Malki-Epshtein L (2018) A parametric study of the effect of roof height and morphology on air pollution dispersion in street canyons. J Wind Eng Ind Aerodyn 175:328–34. https://doi.org/10.1016/j.jweia.2018.02.006

Xing F, Mohotti D, Chauhan K (2018) Study on localised wind pressure development in gable roof buildings having different roof pitches with experiments, RANS and LES simulation models. Build Environ 143:240–257. https://doi.org/10.1016/j.buildenv.2018.07.026

Yassin MF, Al-Rashidi M, Ohba M (2022) Experimental and numerical simulations of air quality in an urban canopy: Effects of roof shapes and atmospheric stability. Atmos Pollut Res 13(12) 101618. https://doi.org/10.1016/j.apr.2022.101618